

RESCEU-04/01  
TU-622  
astro-ph/0105161  
May, 2001

# Cosmic Microwave Background Anisotropy with Cosine-Type Quintessence

Masahiro Kawasaki<sup>(a)</sup>, Takeo Moroi<sup>(b)</sup> and Tomo Takahashi<sup>(b)</sup>

<sup>(a)</sup>*Research Center for the Early Universe, School of Science, University of Tokyo  
Tokyo 113-0033, Japan*

<sup>(b)</sup>*Department of Physics, Tohoku University  
Sendai 980-8578, Japan*

## Abstract

We study the Cosmic Microwave Background (CMB) anisotropies produced by cosine-type quintessence models. In our analysis, effects of the adiabatic and isocurvature fluctuations are both taken into account. For purely adiabatic fluctuations with scale invariant spectrum, we obtain a stringent constraint on the model parameters using the CMB data from COBE, BOOMERanG and MAXIMA. Furthermore, it is shown that isocurvature fluctuations have significant effects on the CMB angular power spectrum at low multipoles in some parameter space, which may be detectable in future satellite experiments. Such a signal may be used to distinguish the cosine-type quintessence models from the tracker-type ones.

# 1 Introduction

It is widely believed that the present cosmological observations are consistent with low density Cold Dark Matter (CDM) models with scale invariant adiabatic density fluctuations. The required energy density of non-relativistic matter is about 30 – 40% of the critical density (i.e.,  $\Omega_m \simeq 0.3 - 0.4$ ). On the other hand, the recent BOOMERanG [1] and MAXIMA [2] experiments on anisotropies of Cosmic Microwave Background (CMB) strongly suggest that our universe is flat, which is also the prediction of the inflationary universe. Thus, there exists dark energy which fills the gap between  $\Omega_m$  and the total energy density  $\Omega_{\text{tot}}$ . Although usually the dark energy is assumed to be the cosmological constant, a slowly evolving scalar field with positive energy can also account for the dark energy [3, 4]. Such a scalar field is called quintessence and has been studied by many authors [5].

At present, the quintessence models are classified into two types; tracker type [3] and cosine type [4]. The former has an attractor-like solution which explains the present dark energy without fine-tuning of the initial condition, while the latter needs tuning of the initial value of the scalar field. This is why the tracker type is favored among cosmologists. However, even for the tracker-type models the model parameters should be fine-tuned to produce the required value of the present quintessence density. In addition, the potential for the tracker field is very exotic and hard to realize in particle physics models.<sup>#1</sup>

One of the observational effects produced by the existence of the quintessence is the CMB anisotropies. In many cases, the quintessence dominates the universe at late times ( $z \sim O(1)$ , with  $z$  being redshift) after the recombination. At that epoch the gravitational potential is changed because the equation of state for quintessence is different from that for non-relativistic matter, which leads to an enhancement of the CMB anisotropies at large angular scales  $l \lesssim 10$  (where  $l$  is the index of spherical harmonics) due to the late-time integrated Sachs-Wolfe effect [7]. The quintessence also changes the locations of the acoustic peaks in the CMB angular power spectrum [8] because the projection of the horizon at last scattering onto the present sky is enlarged compared with models with the cosmological constant.

Furthermore, in the case of cosine-type models, during inflation the quintessence scalar field is effectively massless and has significant quantum fluctuations as large as  $H_{\text{inf}}/2\pi$  where  $H_{\text{inf}}$  is the Hubble parameter during inflation. These fluctuations behave as isocurvature mode and hence the quintessence may have both adiabatic and isocurvature perturbations. The isocurvature fluctuations produce adiabatic ones once their wavelengths enter the horizon. Therefore, we expect larger anisotropies in CMB angular spectrum for cosine-type quintessence models. On the other hand, the tracker field becomes heavy at the sufficiently early epoch and its fluctuations decrease rapidly. Thus, the isocurvature fluctuations are generally negligible for tracker models.<sup>#2</sup>

---

<sup>#1</sup>For model building of the tracker field, see Refs. [6].

<sup>#2</sup>Abramo and Finelli [9] studied the isocurvature fluctuations for tracker-type quintessence models without considering the evolution of the tracker field and its fluctuations during inflation.

In this paper we study the CMB anisotropies produced by quintessence models paying attention to the cosine-type quintessence models. It is shown that the isocurvature fluctuations have significant effects on the CMB angular power spectrum at low multipoles in some parameter space, which may be detectable in future satellite experiments and can be used to distinguish two types of the quintessence models.

This paper is organized as follows. In Section 2, we discuss dynamics of the scalar-field zero mode. In Section 3, behaviors of the fluctuation in the quintessence amplitude are discussed. Then, in Section 4, CMB anisotropy in cosmological models with quintessence is numerically calculated. Section 5 is devoted for conclusions and discussion.

## 2 Dynamics of Scalar-Field Zero Mode

We start our discussion with the behavior of the zero mode of the quintessence field  $Q(t, \vec{x})$ . We denote the zero mode of the quintessence field as  $\bar{Q}(t)$ .

The energy-momentum tensor of the quintessence field is given by

$$T_{\mu\nu} = \partial_\mu Q \partial_\nu Q - \frac{1}{2} [\partial^\alpha Q \partial_\alpha Q + 2V(Q)] g_{\mu\nu}, \quad (2.1)$$

where  $V$  is the quintessence potential. Thus, for  $Q = \bar{Q}$ , the energy density and the pressure of the quintessence field are

$$\rho_Q = \frac{1}{2} \dot{\bar{Q}}^2 + V(\bar{Q}), \quad p_Q = \frac{1}{2} \dot{\bar{Q}}^2 - V(\bar{Q}), \quad (2.2)$$

respectively, where the “dot” represents the derivative with respect to time  $t$ . If the kinetic energy of  $Q$  is negligible compared to the potential energy, the equation of state becomes  $\omega_Q \equiv p_Q/\rho_Q \simeq -1$  and the energy-momentum tensor of the quintessence field behaves like that of the cosmological constant.

The zero mode  $\bar{Q}$  obeys the following equation of motion

$$\ddot{\bar{Q}} + 3H\dot{\bar{Q}} + V'(\bar{Q}) = 0, \quad (2.3)$$

where the “prime” denotes the derivative with respect to  $Q$ . In the very early universe where  $H^2 \gg |V'/\bar{Q}|$ , the slow-roll condition is satisfied and the motion of  $\bar{Q}$  is negligible even if  $\bar{Q}$  is displaced from the minimum of the potential. If the slow-roll condition is satisfied until today, the equation of state  $\omega_Q$  is always very close to  $-1$  and the quintessence is indistinguishable from the cosmological constant. However, this is not always the case. If the effective mass of the quintessence may become larger than the expansion rate,  $Q$  starts to move and  $\omega_Q$  varies. In addition, since the quintessence is a dynamical field, its energy density may fluctuate. Due to these facts, quintessence models may have an interesting consequence in the evolution of the cosmological perturbations, in particular, in the CMB anisotropy. The epoch when the quintessence starts to move is strongly model-dependent. If the slow-roll condition is satisfied until very recently, the quintessence field may provide

significant amount of the energy density with the equation of state close to  $-1$  to the total energy density of the universe. This may be a solution to the “dark energy” problem alternative to the cosmological constant.

In this paper, we consider the cosine-type quintessence potential:

$$V(Q) = \Lambda^4 \left[ 1 - \cos \left( \frac{Q}{f_Q} \right) \right] = 2\Lambda^4 \sin^2 \left( \frac{Q}{2f_Q} \right). \quad (2.4)$$

This type of potential can be generated if the quintessence field is a pseudo Nambu-Goldstone boson. In this class of models, effective mass of the quintessence field is always of  $O(\Lambda^2/f_Q)$ , and is insensitive to the amplitude  $\bar{Q}$ . Requiring that the slow-roll condition for the quintessence field be satisfied until very recently to realize  $\omega_Q \simeq -1$ , the combination  $\Lambda^2/f_Q$  cannot be much larger than the present expansion rate of the universe. Consequently, motion of the quintessence field is negligible for  $z \gg 1$ . Thus, in this class of models, the present energy density of the quintessence field sensitively depends on the initial amplitude.

In the cosine-type models, the present density parameter for the quintessence depends on the following three parameters:  $f_Q$ ,  $\Lambda$ , and the initial amplitude of the quintessence field denoted as  $\bar{Q}_I$ . Assuming the flat universe (i.e.,  $\Omega_m + \Omega_Q = 1$ ), however, one relation among these parameters holds once we fix the present matter density  $\Omega_m = \Omega_{\text{CDM}} + \Omega_b$ , where  $\Omega_{\text{CDM}}$  and  $\Omega_b$  are density parameters for the CDM and baryons, respectively.

In Fig. 1, we plot the contours of constant  $\bar{Q}_I$  which realizes  $\Omega_Q = 0.7$  in the flat universe. Here, we take  $h = 0.65$ , where  $h$  is the present Hubble parameter in units of 100 km/sec/Mpc. Notice that there is no possible value of  $\bar{Q}_I$  consistent with  $\Omega_Q = 0.7$  for  $\Lambda \lesssim 1.9 \times 10^{-12} \text{GeV}$ . This is because the energy density of the quintessence is at most  $2\Lambda^4$  and hence  $\rho_Q$  cannot be large enough if  $2\Lambda^4 < \Omega_Q \rho_c$  with  $\rho_c$  being the critical density of the present universe. When  $2\Lambda^4$  is close to  $\Omega_Q \rho_c$ ,  $\bar{Q}_I$  should be close to  $\pi f_Q$  to realize the relevant value of  $\Omega_Q$ . In this case, motion of the quintessence field is almost negligible and energy density of the quintessence behaves like that of the cosmological constant.

On the contrary, for larger  $\Lambda$ ,  $\bar{Q}_I$  smaller than  $\pi f_Q$  is possible and the motion of the quintessence becomes important. In particular, if  $\Lambda$  becomes large enough, the quintessence oscillates around the minimum of the potential. As one can see, for large enough  $\Lambda$ , the contours have an oscillatory behavior. This can be understood as follows. When the relation  $H \lesssim \Lambda^2/f_Q$  is satisfied, the quintessence field starts to oscillate. If the combination  $\Lambda^2/f_Q$  is large, the oscillation starts earlier epoch and the quintessence field undergoes many oscillations until the present time. We can read off this behavior from Fig. 1. We call the parameter space where the oscillation of the quintessence is significant as “oscillatory region.” When the quintessence field starts to oscillate earlier, it dominates the energy density of the universe from earlier epoch. This has significant implications to the CMB power spectrum.

Evolution of  $\omega_Q$  is also important since it can be quite different from the case of the cosmological constant, in particular when the motion of the quintessence is non-negligible. Typical behaviors of  $\omega_Q$  as a function of the scale factor are shown in Fig. 2. When the

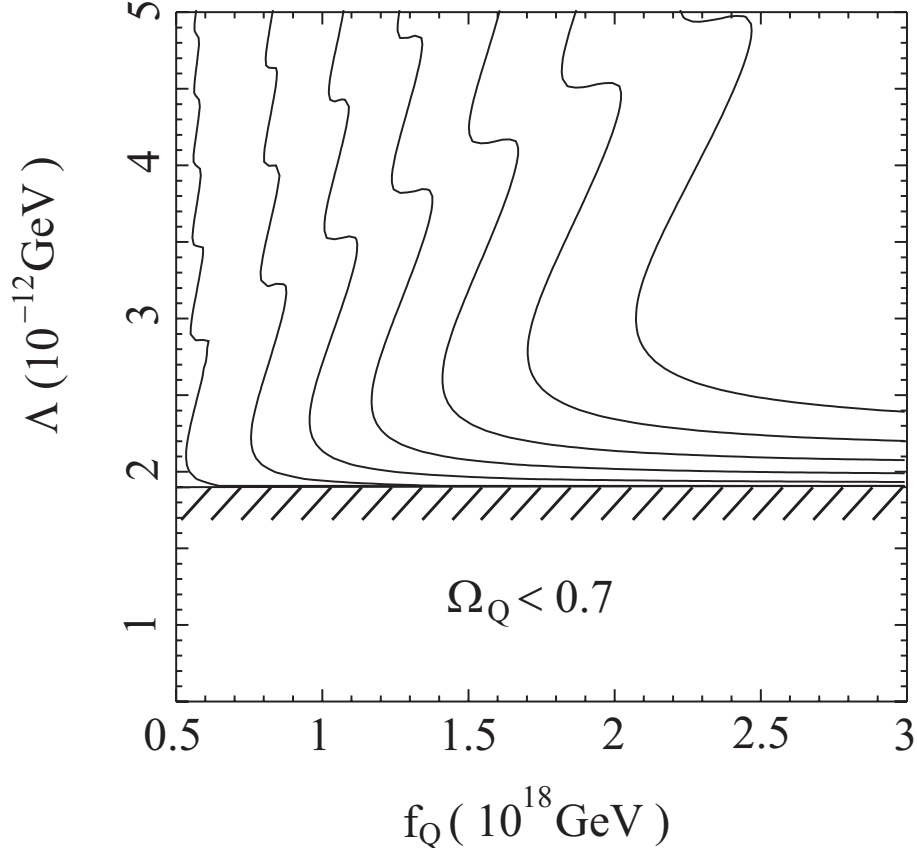


Figure 1: Contours of constant  $\bar{Q}_I/f_Q = 3.0, 2.75, 2.5, 2.25, 2.0, 1.75$  and  $1.5$  from left to right. The value of  $\bar{Q}_I$  is determined such that  $\Omega_Q = 0.7$  in the flat universe (i.e.,  $\Omega_m + \Omega_Q = 1$ ) today. The Hubble parameter is taken to be  $h = 0.65$ . The parameter space  $\Lambda \lesssim 1.9 \times 10^{-12}$  GeV is the region where  $\Omega_Q = 0.7$  cannot be realized for any values of  $\bar{Q}_I$ .

curvature of the potential is smaller than the expansion rate of the universe, evolution of the quintessence can be neglected, and  $\omega_Q \simeq -1$ . On the contrary, when  $H \lesssim \Lambda^2/f_Q$ ,  $\omega_Q$  oscillates between  $-1$  and  $+1$ . If the oscillation is fast enough,  $\omega_Q$  is effectively 0 taking the average over the oscillation. In this case, the scalar field  $Q$  behaves as a non-relativistic matter. If the condition  $H \sim \Lambda^2/f_Q$  is realized in a very recent universe, however, the situation is quite different. In this case, the quintessence field starts to move very recently and the averaged equation of state can be smaller than 0. If so, the scalar field  $Q$  behaves differently from non-relativistic matter and cosmological constant. This may have interesting impacts on the CMB anisotropy as we will see in the following sections.

We also present the evolution of the density parameter of the quintessence:

$$\Omega_Q(t) \equiv \frac{\rho_Q(t)}{\rho_{\text{tot}}(t)}. \quad (2.5)$$

Like the case of the cosmological constant,  $\Omega_Q(t)$  is negligibly small in the early uni-

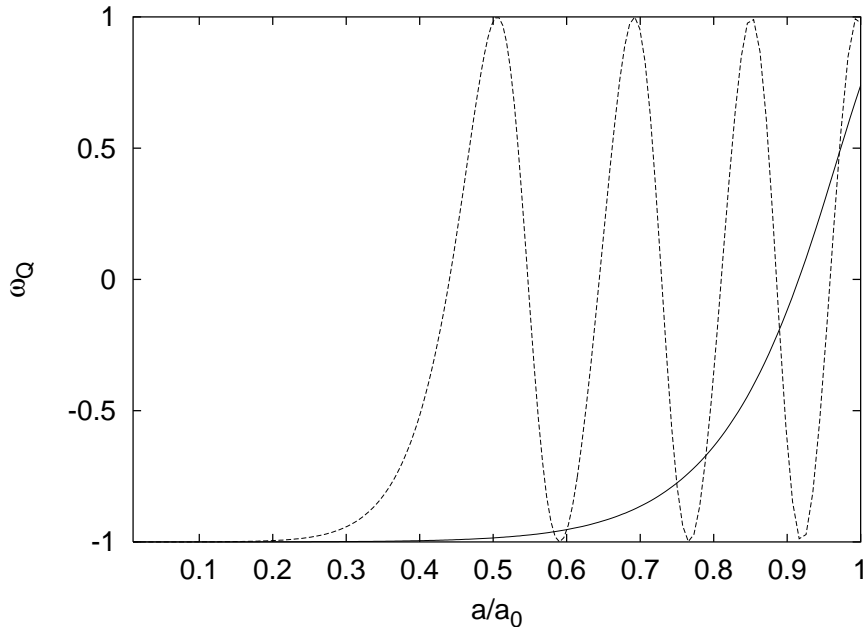


Figure 2: Evolution of the equation of state  $\omega_Q$  for (a)  $f_Q = 5.0 \times 10^{17}$  GeV and  $\Lambda = 2.3 \times 10^{-12}$  GeV (solid line), and (b)  $f_Q = 5.0 \times 10^{17}$  GeV and  $\Lambda = 4.0 \times 10^{-12}$  GeV (dashed line). Here, we take  $h = 0.65$ ,  $\Omega_m = 0.3$  and  $\Omega_Q = 0.7$ .

verse. When  $z \sim O(1)$ , however,  $\Omega_Q(t)$  becomes close to 1 and the energy density of the quintessence becomes sizable. One interesting feature is that, if the slow-roll condition does not hold, the behavior of  $\Omega_Q(t)$  is quite different from that of the cosmological constant. In particular, as  $\Lambda$  becomes larger,  $\rho_Q$  becomes the dominant component of the total energy density at earlier stage.

The observations of Type Ia Supernovae suggest that  $\omega_Q$  is less than about  $-0.7$  at  $z \lesssim 1$  for  $\Omega_m = 0.3$  [10]. However, it was pointed that there exist some possible systematic errors such as dust absorption and/or evolution effect [11]. Therefore, in this paper, we do not use the supernovae data to obtain constraints on the quintessence models.

### 3 Fluctuation in the Quintessence Field

Since the quintessence is a scalar field, its amplitude may have position-dependent fluctuations. To investigate its behavior, we decompose the  $Q$  field as

$$Q(t, \vec{x}) = \bar{Q}(t) + q(t, \vec{x}), \quad (3.1)$$

where  $q$  is the perturbation of the amplitude of the quintessence field. Hereafter, we study the evolution of  $q$  using the linearized equations for the perturbations.

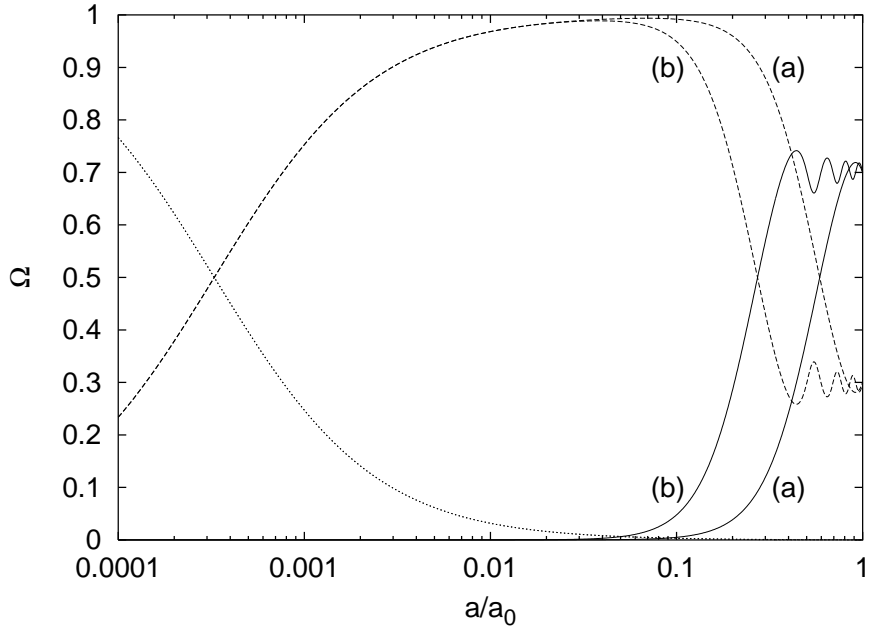


Figure 3: Evolution of the density parameters. We show  $\Omega_Q$  (solid line),  $\Omega_m$  (dashed line) and  $\Omega_{\text{radiation}}$  (dotted line). Cosmological and model parameters are the same as Fig. 2

The equation of motion for  $q$  is, in the synchronous gauge,

$$\ddot{q} + 3H\dot{q} - \left(\frac{a}{a_0}\right)^{-2} \partial_i^2 q + V''(\bar{Q})q = -\frac{1}{2}\dot{h}\dot{Q}, \quad (3.2)$$

where  $\partial_i$  is the derivative with respect to the comoving coordinate  $x^i$ . Here, the perturbed line element in the synchronous gauge is given by

$$ds^2 = -dt^2 + \left(\frac{a}{a_0}\right)^2 (\delta_{ij} + h_{ij}) dx^i dx^j = \left(\frac{a}{a_0}\right)^2 [-d\tau^2 + (\delta_{ij} + h_{ij}) dx^i dx^j], \quad (3.3)$$

where  $\tau$  is the conformal time coordinate,  $a$  the scale factor at time  $t$ ,  $a_0$  the scale factor at the present time, and  $h$  is the trace of  $h_{ij}$ .<sup>#3</sup> In the momentum space, we expand  $h_{ij}$  as

$$h_{ij}(t, \vec{x}) = \int \frac{d^3k}{(2\pi)^{3/2}} \left[ \frac{k_i k_j}{k^2} h(\vec{k}, t) + \left( \frac{k_i k_j}{k^2} - \frac{1}{3} \delta_{ij} \right) 6\eta(\vec{k}, t) \right] e^{i\vec{k}\vec{x}}, \quad (3.4)$$

with  $k^2 = k_i k^i$ . Notice that, in the momentum space, the gauge-invariant variable  $\Psi$  is related to  $h$  and  $\eta$  as

$$\Psi(k) = \frac{1}{2k^2} \left[ \frac{\partial^2 h(k)}{\partial \tau^2} + 6 \frac{\partial^2 \eta(k)}{\partial \tau^2} + \frac{1}{a} \frac{\partial a}{\partial \tau} \left( \frac{\partial h(k)}{\partial \tau} + 6 \frac{\partial \eta(k)}{\partial \tau} \right) \right]. \quad (3.5)$$

<sup>#3</sup>The metric perturbation  $h$  should not be confused with the Hubble parameter.

Numerically, we checked that the terms proportional to the derivatives of  $\eta$  are subdominant relative to contributions from the derivatives of  $h$ .

There are two origins of non-vanishing  $q$  at the present time. As indicated in Eq. (3.2), the metric perturbation  $h$  generates non-vanishing  $q$  even if  $q$  initially vanishes. We call this fluctuation as ‘‘adiabatic fluctuation’’ of the quintessence field. Let us briefly discuss how the adiabatic fluctuation of  $q$  is generated. For this purpose, it is instructive to consider the matter-dominated universe even though, in our case, the energy density of the present universe has significant contribution from the quintessence. Fluctuation for the scale smaller than the horizon scale oscillates and damps, so we consider  $q(k)$  which has larger physical momentum than the expansion rate of the universe. Then, the third term in the left-hand side of Eq. (3.2), i.e.,  $\partial_i^2 q$ , is negligible. In solving Eq. (3.2), it is convenient to use the fact that  $\Psi$  is (almost) constant of time in matter-dominated epoch. In addition, for the zero mode, we use the slow-roll condition to derive  $\dot{\bar{Q}} \simeq -\frac{2}{9}(V'/H)$ . With these informations,  $q(k)$  at a given time  $t$  is, in the synchronous gauge,

$$q(k) = \frac{3}{88}(a_0/a)^2 k^2 V' \Psi(k) t^4, \quad (3.6)$$

which is proportional to  $t^{8/3}$ . In the realistic situation, however, some of the approximations used to derive the above relation may fail. Therefore, in our analysis, we numerically solve the equation of motion for the quintessence field to obtain  $q(k)$ .

The second origin is the primordial perturbation in the quintessence amplitude generated in the very early universe, probably during the inflation. We call this fluctuation as ‘‘isocurvature fluctuation,’’ since the total density fluctuation and the potential  $\Psi$  vanish as  $a \rightarrow 0$  if this is the only source of the fluctuation in the early universe.

The isocurvature mode may arise due to the quantum fluctuation during the inflation. In order to calculate the expected fluctuation generated during the inflation, we quantize the scalar field in the de Sitter background. Identifying  $q$  as a field operator, it can be expanded as

$$q(t, \vec{x}) = \int \frac{d^3k}{(2\pi)^{3/2}} \left[ \hat{a}_k \varphi_k(\tau) e^{i\vec{k}\vec{x}} + \hat{a}_k^\dagger \varphi_k^\dagger(\tau) e^{-i\vec{k}\vec{x}} \right], \quad (3.7)$$

where, assuming minimally coupled Lagrangian for the quintessence field, the mode function is given by

$$\varphi_k(\tau) = \frac{\sqrt{\pi}}{2} H_{\text{inf}} \tau^{3/2} H_\nu^{(1)}(k\tau), \quad (3.8)$$

with  $H_\nu^{(1)}$  being the Hankel function of the first kind and

$$\nu^2 = \frac{9}{4} - \frac{m_q^2}{H_{\text{inf}}^2}. \quad (3.9)$$

Here,  $m_q$  is an effective mass for the quintessence field during the inflation, and  $H_{\text{inf}}$  is the expansion rate of the de Sitter background.

Adopting the Bunch-Davis vacuum [12], the operators  $\hat{a}_k$  and  $\hat{a}_k^\dagger$  are identified as the creation and annihilation operators, respectively, and satisfy the following commutation relations:

$$[\hat{a}_k, \hat{a}_l] = [\hat{a}_k^\dagger, \hat{a}_l^\dagger] = 0, \quad [\hat{a}_k, \hat{a}_l^\dagger] = \delta^{(3)}(\vec{k} - \vec{l}). \quad (3.10)$$

Using these relations, the equal-time two-point function for  $q$  is given as

$$\begin{aligned} G(t, \vec{x}; t, \vec{y}) &\equiv \langle 0|q(t, \vec{x})q(t, \vec{y})|0\rangle \\ &= \frac{\pi}{4H_{\text{inf}}} \int \frac{d^3k_{\text{phys}}}{(2\pi)^3} |H_\nu^{(1)}(k_{\text{phys}}/H_{\text{inf}})|^2 e^{i\vec{k}_{\text{phys}}(\vec{x}_{\text{phys}} - \vec{y}_{\text{phys}})}, \end{aligned} \quad (3.11)$$

where physical momentum  $k_{\text{phys}}$  is related to the comoving one  $k$  as

$$k_{\text{phys}} = (a_0/a)k, \quad (3.12)$$

and  $\vec{x}_{\text{phys}} = (a/a_0)\vec{x}$ . During the inflation, the present horizon scale is far outside of the horizon, and hence we are interested in the behavior of  $G(t, \vec{x}; t, \vec{y})$  with  $|\vec{x}_{\text{phys}} - \vec{y}_{\text{phys}}| \gg H_{\text{inf}}^{-1}$ . In other words, we only need an information of the integrand with  $k_{\text{phys}} \ll H_{\text{inf}}$ . Denoting

$$G(t, \vec{x}; t, \vec{y}) = \int \frac{dk_{\text{phys}}}{k_{\text{phys}}} |\tilde{q}(k)|^2 e^{i\vec{k}_{\text{phys}}(\vec{x}_{\text{phys}} - \vec{y}_{\text{phys}})}, \quad (3.13)$$

$\tilde{q}(k)$  for small  $k$  is given by

$$\tilde{q}(k) = \frac{2\sqrt{\pi}}{\Gamma(-\nu + 1) \sin \nu\pi} \left( \frac{k_{\text{phys}}}{2H_{\text{inf}}} \right)^{-(\nu-3/2)} \frac{H_{\text{inf}}}{2\pi}. \quad (3.14)$$

For the case where  $m_q \gtrsim H_{\text{inf}}$ ,  $|(k_{\text{phys}}/2H_{\text{inf}})^{-(\nu-3/2)}| \ll 1$  since we are interested in modes with  $k_{\text{phys}} \ll H_{\text{inf}}$ . (Notice that, in most of the inflation models, the COBE scale corresponds to  $\ln(H_{\text{inf}}/k_{\text{phys}}) \sim 50 - 60$ .) Thus, for the quintessence models with relatively large (effective) mass during the inflation, the primordial fluctuation in  $\tilde{q}$  is extremely suppressed relative to  $H_{\text{inf}}$ . If the mass of the quintessence is light, however,  $\nu$  becomes close to  $3/2$  and the suppression factor may become negligible. In this limit,  $\tilde{q}(k)$  is given by

$$\tilde{q}(k) \simeq \left( \frac{k_{\text{phys}}}{2H_{\text{inf}}} \right)^{2m_q^2/3H_{\text{inf}}^2} \frac{H_{\text{inf}}}{2\pi}, \quad (3.15)$$

and hence  $\tilde{q} \simeq H_{\text{inf}}/2\pi$  for  $m_q \ll H_{\text{inf}}$ . In order to avoid a significant suppression for the primordial perturbation,  $m_q/H_{\text{inf}} \lesssim 0.1 - 0.2$  is enough. In addition, notice that, for  $m_q/H_{\text{inf}} \ll 1$ , the resultant  $\tilde{q}$  is expected to be almost scale independent; the only source of the scale dependence is a minor variation of the expansion rate  $H_{\text{inf}}$  during the inflation. In the following discussion, we neglect the scale dependence of  $\tilde{q}$ .

It is convenient to consider the ratio of the primordial value of  $\tilde{q}$  to that of the gauge-invariant variable  $\tilde{\Psi}$  at the radiation-dominated universe:<sup>#4</sup>

$$r_q \equiv \frac{\tilde{q}}{M_* \tilde{\Psi}}, \quad (3.16)$$

where  $M_* \simeq 2.4 \times 10^{18}$  GeV is the reduced Planck scale, and  $\tilde{\Psi}$  is defined as  $\langle \Psi(\vec{x})\Psi(\vec{y}) \rangle = \int d \ln k |\tilde{\Psi}(k)|^2 e^{i\vec{k}(\vec{x}-\vec{y})}$ .

Solving the dynamics of the inflaton during the inflation, we obtain  $\tilde{\Psi}$  at the radiation-dominated era [13]

$$\tilde{\Psi} = \frac{4}{9} \left( \frac{H_{\text{inf}}^2}{2\pi|\dot{\chi}|} \right), \quad (3.17)$$

where  $\chi$  is the inflaton field. Using the slow-roll condition for  $\chi$ , and also using  $\tilde{q} \simeq H_{\text{inf}}/2\pi$ , we obtain

$$r_q \simeq \frac{9 M_* V'_{\text{inf}}}{4 V_{\text{inf}}}, \quad (3.18)$$

where  $V_{\text{inf}}$  is the inflaton potential and  $V'_{\text{inf}}$  is its derivative with respect to the inflaton field.<sup>#5</sup> For example, for the chaotic inflation with  $V_{\text{inf}} \propto \chi^p$  with  $p$  being an integer,  $r_q$  is given by

$$r_q|_{\text{chaotic}} = \frac{9pM_*}{4\chi(k_{\text{COBE}})}, \quad (3.19)$$

where  $\chi(k_{\text{COBE}})$  represents the inflaton amplitude at the time when the COBE scale crosses the horizon. Numerically, we found  $r_q \simeq 0.3 - 0.6$  for  $p = 2 - 10$ . Since the ratio  $r_q$  generically depends on the model of the inflation, we treat  $r_q$  as a free parameter in our analysis.

Notice that, in our analysis, we treat  $\tilde{\Psi}$  and the fluctuation in the quintessence amplitude as random Gaussian variables. In particular, no correlation is assumed among these quantities. Thus,  $r_q$  given in Eq. (3.16) should be understood as the ratio of the expectation values of  $\tilde{q}$  and  $\tilde{\Psi}$ , and we add adiabatic and isocurvature contributions in quadrature in calculating the CMB anisotropy.

---

<sup>#4</sup>In our analysis, we only consider the case with scale-independent primordial fluctuation, and  $r_q$  is treated as a scale-invariant quantity. When  $r_q$  has a scale dependence via  $\tilde{\Psi}$  and/or  $\tilde{q}$ ,  $r_q(k)$  for the present horizon scale becomes the most important since the quadrupole anisotropy is most strongly affected by the isocurvature mode as will be shown below.

<sup>#5</sup>If  $f_Q$  during the inflation, which is denoted as  $f_Q^{(\text{inf})}$ , is smaller than the present value,  $r_q$  is enhanced by the factor  $f_Q/f_Q^{(\text{inf})}$ . This may happen if the quintessence is a pseudo Nambu-Goldstone boson; in that case  $f_Q$  is given by a vacuum expectation value of a (real) scalar field, which varies if the scalar potential is deformed during the inflation.

Now, we consider the evolution of the isocurvature fluctuation after the inflation. The evolution of the isocurvature mode is well described by the equation Eq. (3.2) with neglecting the right-hand side (i.e.,  $h = 0$ ). This is because, when the energy density of the quintessence is negligible, the metric perturbation  $h$  is insensitive to the fluctuation in the quintessence and we can neglect the right-hand side of Eq. (3.2) in studying the isocurvature perturbation. In the early universe, this is the case for the cosine-type quintessence. Let us first consider the case with large wavelength (i.e.,  $k_{\text{phys}} \ll H$ ). In this case, the third term in Eq. (3.2) is irrelevant. By neglecting the right-hand side of Eq. (3.2),  $q$  behaves like a harmonic oscillator with effective mass-squared  $V''(\bar{Q})$  in the expanding background. Then, we can imagine two typical cases. If the effective mass is much smaller than the expansion rate of the universe, the slow-roll condition is satisfied for  $q$ . In this case,  $q$  keeps its initial value until the expansion rate of the universe becomes comparable to the effective mass of the quintessence field. This is the case for the cosine-type quintessence models in the early universe. On the contrary, if the effective mass becomes comparable to or larger than the expansion rate,  $q$  is under a damped oscillation. In fact, for typical tracker models with inverse power potential or exponential potential (like  $V \propto 1/Q^p$  with  $p \geq 1$  or  $V \propto e^{M_*/Q}$ ),  $|q|^2$  is proportional to  $a^{-1}$ . Thus, in the tracker case, primordial perturbation generated during the inflation is dumped when the tracker field evolves down to the attractor point.

As the universe expands after the inflation, the horizon expands more rapidly than the physical scale, and hence all the momentum scales relevant to our discussion eventually enter the horizon. Once the scale enters the horizon, the spatial derivative term cannot be neglected. The energy density of such modes behaves like that of relativistic matter, and hence it decreases as  $a^{-4}$ . Thus, once  $k_{\text{phys}} \sim H$  is realized,  $\tilde{q}(k)$  decreases as  $a^{-1}$ .

So far, we have seen that the perturbation in the quintessence amplitude  $q$  can be generated by several sources. If  $q$  is non-vanishing, the energy density of the quintessence field fluctuates. The energy density, pressure, and momentum perturbations of the quintessence are given by

$$\delta\rho_Q = \dot{\tilde{Q}}\dot{q} + V'q, \quad \delta p_Q = \dot{\tilde{Q}}\dot{q} - V'q, \quad (\rho_Q + p_Q)(v_Q)_i = -\left(\frac{a_0}{a}\right)\dot{\tilde{Q}}\frac{\partial q}{\partial x^i}, \quad (3.20)$$

respectively. This will affect the density perturbation of the universe and may change the behavior of the CMB anisotropy, as will be discussed in the following section.

## 4 Numerical Results

### 4.1 Outline of the Analysis

To study the CMB anisotropy in models with quintessence, we solve the perturbed Einstein equation coupled to the equation of motion of the quintessence field (as well as evolution equations of other components like CDM, photon, baryon, and neutrinos). Then, we compare the theoretical prediction of the CMB anisotropy with observations.

As a first step, the total density and pressure perturbations are derived by adding the quintessence contributions. Notice that these quantities affect the evolution of the metric perturbations. Then, we solve the evolution equations for the perturbations including the quintessence contributions. Evolution of  $\bar{Q}(t)$  is simultaneously solved since it affects the expansion rate and the equation of state at each epoch. In particular, for the perturbed part of the equations, we modify the **CMBFAST** package [14] to include the quintessence contributions. Then, we calculate the CMB anisotropy for the  $l$ -th multipole  $C_l$ , which is defined as

$$\langle \Delta T(\vec{x}, \vec{\gamma}) \Delta T(\vec{x}, \vec{\gamma}') \rangle = \frac{1}{4\pi} \sum_l (2l+1) C_l P_l(\vec{\gamma} \cdot \vec{\gamma}'), \quad (4.1)$$

where  $\Delta T(\vec{x}, \vec{\gamma})$  is the temperature fluctuation of the CMB pointing to the direction  $\vec{\gamma}$ , and the average is over the position  $\vec{x}$ .

Since we have not specified any particular model of inflation which determines the normalization of the CMB anisotropy, over-all normalization of  $C_l$  is undetermined at this stage. We treat the normalization of the CMB anisotropy as a free parameter to make our study model-independent. Thus, in our analysis, the normalization of the CMB anisotropy is fixed so that the theoretical prediction has the best fit to the observational data. We denote the actual CMB anisotropy  $C_l$  as

$$C_l = N \bar{C}_l, \quad (4.2)$$

where  $\bar{C}_l$  is the normalization-free CMB anisotropy and  $N$  is the normalization factor which minimizes the  $\chi^2$  defined below.

Since accurate measurements of the CMB anisotropy have been performed by COBE [15], BOOMERanG [1] and MAXIMA [2], we can constrain the quintessence models by comparing the theoretical prediction on  $C_l$  with observations. For this purpose, we calculate the goodness-of-fit parameter  $\chi^2 = -2 \ln L$ , where  $L$  is the likelihood function. (We call this parameter as  $\chi^2$ , since it reduces to the usual  $\chi^2$ -variable for a Gaussian.) In our statistical analysis, following Ref. [16], we use the offset lognormal approximation to derive  $\chi^2$  as

$$\chi^2 = \sum_{BB'} (Z_B^{\text{th}} - Z_B^{\text{obs}}) M_{BB'}^Z (Z_{B'}^{\text{th}} - Z_{B'}^{\text{obs}}), \quad (4.3)$$

where the summation is over the band powers obtained by COBE, BOOMERanG and MAXIMA. The quantity  $Z_B^{\text{obs}}$  contains informations from the observations as

$$Z_B^{\text{obs}} = \ln(D_B + x_B), \quad (4.4)$$

where  $D_B$  is the observed band power in  $B$ -th band and  $x_B$  is the offset correction, and  $M_{BB'}^Z$  is given by

$$M_{BB'}^Z = M_{BB'}^D (D_B + x_B)(D_{B'} + x_{B'}), \quad (4.5)$$

where  $M_{BB'}^D$  is the weight matrix for the band powers  $D_B^2$ . (In Eq. (4.5), no summation over  $B$  nor  $B'$  is implied.) In addition,  $Z_B^{\text{th}}$  is written as

$$Z_B^{\text{th}} = \ln \left( N \sum_l u_\alpha f_{Bl} \bar{C}_l + x_B \right), \quad (4.6)$$

where  $f_{Bl}$  is the filter function and  $u_\alpha$  is the calibration parameter.<sup>#6</sup> In our analysis, we neglect the calibration uncertainty in COBE and assume flat (top-hat) distributions of  $u_{\text{BOOMERanG}} = 1 \pm 0.2$  and  $u_{\text{MAXIMA}} = 1 \pm 0.08$  [17]. For a given set of  $\bar{C}_l$ , we vary  $N$ ,  $u_{\text{BOOMERanG}}$ , and  $u_{\text{MAXIMA}}$  to minimize the  $\chi^2$  parameter. In our numerical calculations, we use RADPACK package [18] to calculate  $\chi^2$ , which is based on 24, 12, and 10 band powers from COBE, BOOMERanG, and MAXIMA, respectively.

## 4.2 Adiabatic Fluctuation

Now, we are at the position to study the CMB anisotropy in models with quintessence. In this subsection, we consider the effects of the adiabatic perturbation so we take  $r_q = 0$ .

In Fig. 4, we first show the CMB angular power spectrum. Here, the cosmological parameters are taken to be  $h = 0.65$ ,  $\Omega_m = 0.3$ ,  $\Omega_b h^2 = 0.019$ , and the initial spectral index is  $n = 1$ . We assume that there are no tensor mode contributions. The normalization factor  $N$  is chosen such that  $\chi^2$  is minimized.

Some of the interesting features of the CMB angular power spectrum are discussed in order. First, let us consider the locations of the acoustic peaks. The locations of the peaks depend on two quantities, the sound horizon at last scattering and the angular diameter distance to the last scattering surface. Approximately, the  $l$ -th multipole picks up scales around  $l \sim kr_\theta(\tau_*)$  where  $r_\theta(\tau_*)$  is the angular diameter distance to the last scattering surface [20]. The  $n$ -th peak in the temperature power spectrum is located at the scale  $k_n$  which satisfies  $k_n r_s(\tau_*) = n\pi$ , where  $r_s(\tau_*)$  is the sound horizon at last scattering. So the location of  $n$ -th peak in the  $l$  space is estimated as

$$l_n \simeq \frac{r_\theta(\tau_*)}{r_s(\tau_*)} n\pi. \quad (4.7)$$

Since the behavior of the cosine-type quintessence is almost the same as that of the cosmological constant until very recently, the sound horizon at last scattering is the same in both cases. The angular diameter distance in the quintessence model is, however, different from that in the  $\Lambda$ CDM models. Since the quintessence models provides larger total energy density of the universe than the  $\Lambda$ CDM models in the earlier epoch, the angular diameter distance in the quintessence model becomes smaller than that in the  $\Lambda$ CDM models. As we can see from Fig. 4, the location of the peaks is shifted to lower multipole  $l$  for the quintessence models. If we take a parameter in the oscillatory region, this feature

---

<sup>#6</sup>In our analysis, we assume that the calibration uncertainty  $u_\alpha$  has a flat distribution. Therefore,  $\chi^2$  given in Eq. (4.3) does not contain contributions from the calibration uncertainties.

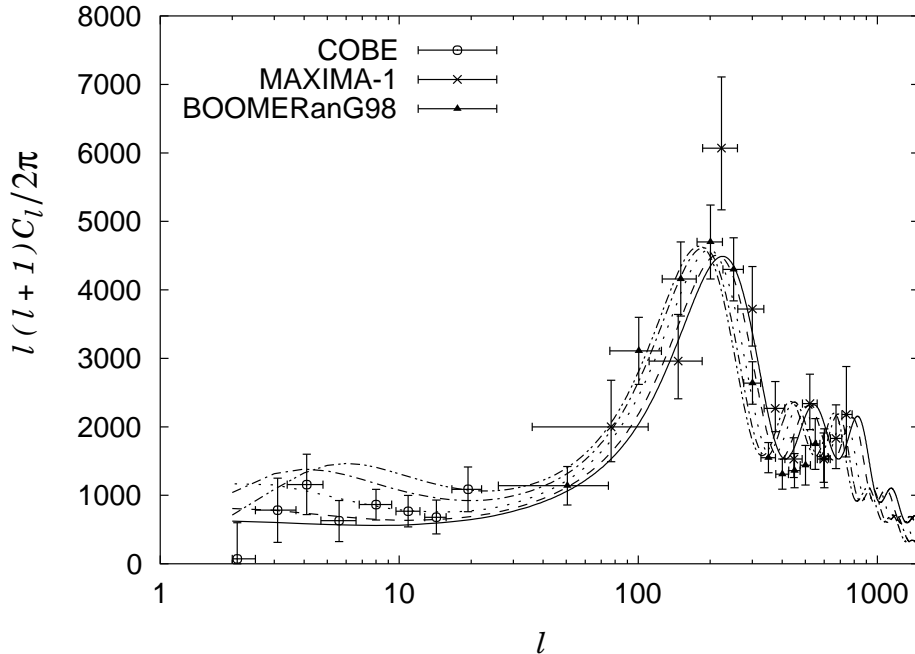


Figure 4: The CMB angular power spectrum  $l(l+1)C_l/2\pi$  in models with cosine-type quintessence. The parameters we take here,  $f_Q = 1.8 \times 10^{18}$  GeV,  $\Lambda = 2.4 \times 10^{-12}$  GeV (dashed line),  $\Lambda = 3.0 \times 10^{-12}$  GeV (dotted line),  $\Lambda = 4.0 \times 10^{-12}$  GeV (dash-dot line),  $\Lambda = 5.0 \times 10^{-12}$  GeV (dash-dot-dot line). For comparison, we also show the cosmological constant case (solid line). Here, the cosmological parameters are taken to be  $h = 0.65$ ,  $\Omega_m = 0.3$ ,  $\Omega_b h^2 = 0.019$ , and the initial spectral index is  $n = 1$ . We also show the data points from COBE, BOOMERanG, and MAXIMA. (For COBE, we use the reduced data set given in Ref. [19].)

becomes more prominent. As  $\Lambda$  becomes larger, more energy density exists in the early universe since some fraction of the energy density of the quintessence damps away during the oscillation.

Next let us consider the height of the acoustic peaks. Since the energy density of the quintessence becomes dominant when  $z \sim O(1)$ , the late time integrated Sachs-Wolfe (ISW) effect enhances low multipoles. Such an enhancement may be more effective in the quintessence models than in the  $\Lambda$ CDM models since, in the quintessence case, the “dark energy” (i.e., the quintessence) may dominate the universe earlier than in the  $\Lambda$ CDM case. As a result, with the COBE normalization, the height of the first peak becomes lower. On the contrary, since the quintessence becomes the dominant component of the universe only at later epoch, pattern of the acoustic oscillation before the recombination does not change compared to  $\Lambda$ CDM models. Therefore, ratios of the height of the first peak to those of higher peaks are the same as  $\Lambda$ CDM models.

There is another point which should be addressed. If we take a parameter in the deep oscillatory region, we can see a bump in the low multipole region. At low multipoles, the

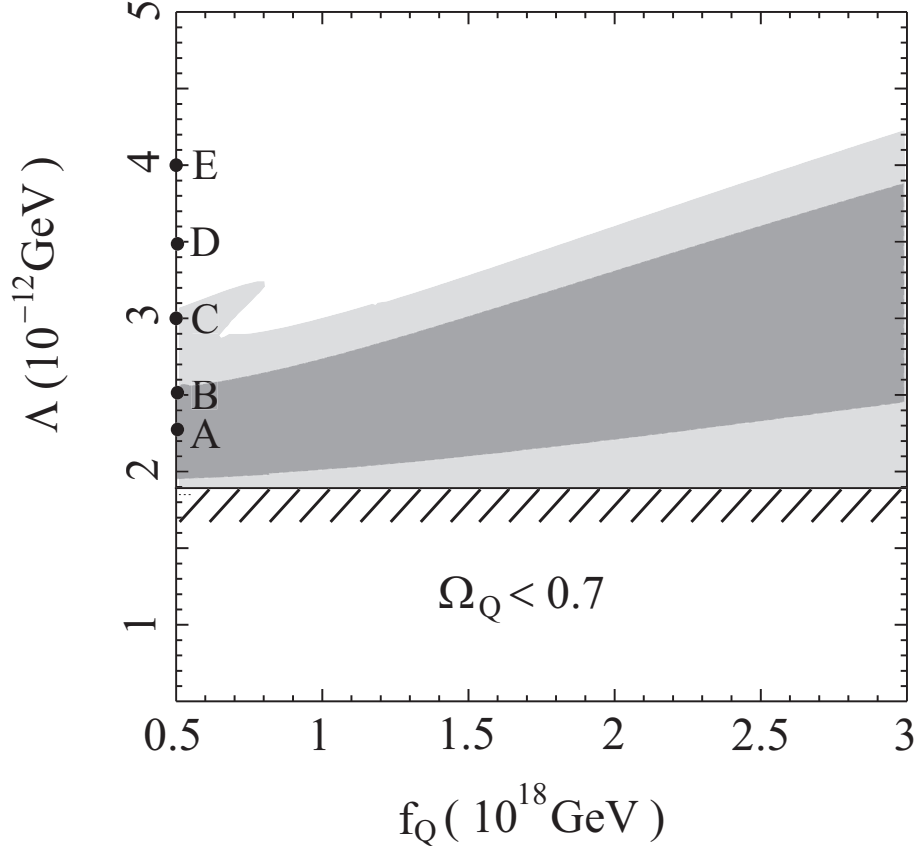


Figure 5: Constraints on the parameters  $\Lambda$  and  $f_Q$ . The lightly shaded regions are for  $\chi^2 \leq 68.7$ , and the darkly shaded region is for  $\chi^2 \leq 60.5$ . The cosmological parameters are taken to be  $h = 0.65$ ,  $\Omega_m = 0.3$ ,  $\Omega_b h^2 = 0.019$ , and the initial spectral index is  $n = 1$ . The Points A – E will be used as representative points in the later discussion.

late time ISW effect is important for the temperature fluctuations in  $\Lambda$ CDM models or in the quintessence models. The ISW effect is originated from the decay of the gravitational potential at the time of the quintessence (or the cosmological constant) domination. Before the quintessence field starts to oscillate, the equation of state of the quintessence field is almost  $-1$ , and hence this epoch is like the cosmological-constant-dominated epoch. After the quintessence starts to oscillate, however,  $\omega_Q$  approaches to 0 and hence the quintessence field behaves like a matter component. Then, the gravitational potential  $\Psi$  takes a constant value again, and the ISW effect becomes ineffective. Consequently, the bump in low multipoles shows up. Notice that the location of this bump corresponds to the transition scale from the slow-roll epoch to the oscillatory epoch.

Now we discuss constraints on the cosine-type quintessence models from the observations of COBE, BOOMERanG and MAXIMA. Following the prescription given in the previous subsection, we calculate the goodness-of-fit parameter  $\chi^2$  as a function of  $f_Q$  and  $\Lambda$ . Based on this  $\chi^2$  variable, constraints on the parameter  $f_Q$  and  $\Lambda$  are shown in Fig.

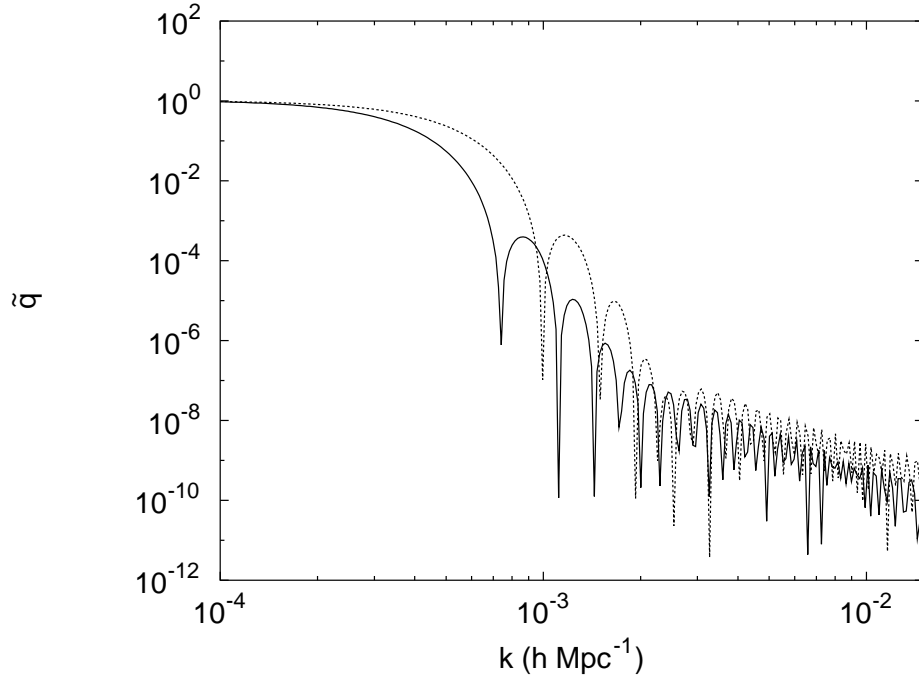


Figure 6:  $\tilde{q}$  as a function of  $k$ .  $\tilde{q}$  is normalized to unity at large scale (small  $k$ ). Here, the model parameters are taken to be  $f_Q = 5.0 \times 10^{17}$  GeV and  $\Lambda = 2.3 \times 10^{-12}$  GeV (solid line),  $f_Q = 5.0 \times 10^{17}$  GeV and  $\Lambda = 3.5 \times 10^{-12}$  GeV (dashed line) .

5. Here, we show the region consistent with  $\chi^2 \leq 60.5$  and  $\chi^2 \leq 68.7$ , which correspond to 95 % and 99 % C.L. allowed region for the  $\chi^2$ -statistics with 44 degrees of freedom, respectively.

When we take a parameter in the oscillatory regions, the quintessence field becomes dominant component of the universe at earlier epoch. Namely the late time ISW effect becomes large and the angular diameter distance to the last scattering surface becomes smaller as mentioned before. Therefore, if  $\Lambda$  is significantly large, the late time ISW effect enhances angular power spectrum at low multipoles. As a result, the heights of the acoustic peaks are suppressed relative to  $C_l$  with small  $l$ .

### 4.3 Isocurvature Mode

Now, let us consider the effect of the isocurvature fluctuation which may be generated in the very early universe (like during the inflation).

Before discussing the CMB anisotropy generated by the isocurvature mode, let us first study the behavior of the fluctuation in the quintessence amplitude  $\tilde{q}$ . Since the isocurvature contribution to  $C_l$  does not interfere with the adiabatic one, studying the purely isocurvature case is enough to understand the effect of the isocurvature perturbation.

In Fig. 6, we show the scale dependence of  $\tilde{q}$ . As one can see,  $\tilde{q}(k)$  changes its behavior

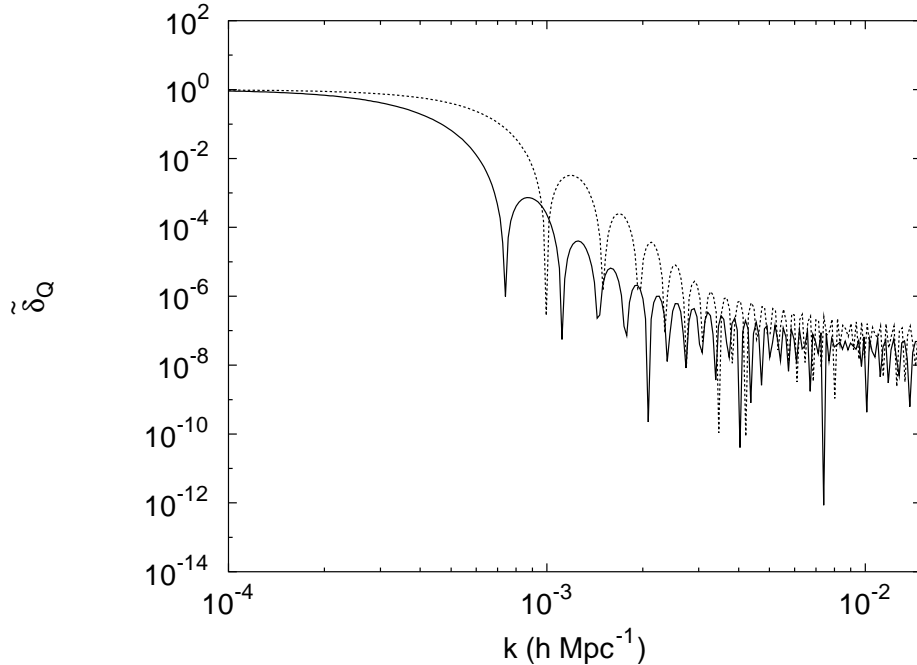


Figure 7:  $\tilde{\delta}_Q$  as a function of  $k$ .  $\tilde{\delta}_Q$  is normalized to unity at large scale (small  $k$ ). Cosmological and model parameters are the same as Fig. 6.

at the scale which is slightly smaller than the present horizon scale:  $\tilde{q}(k)$  is almost constant for small  $k$  while  $\tilde{q}(k)$  is suppressed for large  $k$ . This behavior is understood as follows. When the slow-roll condition is satisfied for the quintessence, fluctuation for the scale larger than the horizon scale takes its initial value. On the contrary, for  $k_{\text{phys}} \gtrsim H$ ,  $\tilde{q}$  behaves like an oscillator with frequency  $\sim k_{\text{phys}}$ , and the fluctuation red-shifts as the universe expands. Due to the red shift, the magnitude of  $\tilde{q}$  is approximately proportional to  $k^{-2}$  and  $k^{-1}$  for modes entering the horizon in the matter-dominated and radiation-dominated universe, respectively. If the slow-roll condition is satisfied until the present universe,  $\tilde{q}(k)$  for  $k_{\text{phys}} \gtrsim H_0$  is suppressed.

If  $m_{\text{eff}} \sim \Lambda^2/f_Q \gtrsim H_0$ , however, the quintessence field may start to oscillate at some stage of the universe. (We call the horizon scale at this epoch as  $1/k_{\text{phys}}^{(\text{osc})}$ .) Once the quintessence starts to oscillate with frequency  $m_{\text{eff}}$ , then all the modes universally damps as far as  $k_{\text{phys}} \lesssim m_{\text{eff}}$ . Thus, for  $k_{\text{phys}} \lesssim k_{\text{phys}}^{(\text{osc})}$ ,  $\tilde{q}$  is independent of  $k$ . On the contrary, modes with  $k_{\text{phys}} \gtrsim k_{\text{phys}}^{(\text{osc})}$  acquire extra suppression as we discussed, and  $\tilde{q}$  for such a small scale becomes smaller. In our analysis we only consider cases where  $1/k_{\text{phys}}^{(\text{osc})}$  is close to the present horizon scale. In those cases, the isocurvature fluctuation in the quintessence field dominantly affects  $C_l$  with small  $l$ , as we will see below.

In Fig. 7, we also plot the scale dependence of the energy density perturbation in the

	$r_q = 0$	$r_q = 0.5$	$r_q = 1$	$r_q = 1.5$	$r_q = 2$
A	1.31	1.31	1.32	1.33	1.34
B	1.45	1.46	1.48	1.51	1.56
C	1.15	1.26	1.61	2.18	2.98
D	0.84	1.33	2.80	5.25	8.69
E	0.62	1.93	5.86	12.41	21.58

Table 1:  $C_2/C_{10}$  for several values of  $r_q$ . We take  $f_Q = 5 \times 10^{17}$  GeV, and (A)  $\Lambda = 2.3 \times 10^{-12}$  GeV, (B)  $\Lambda = 2.5 \times 10^{-12}$  GeV, (C)  $\Lambda = 3.0 \times 10^{-12}$  GeV, (D)  $\Lambda = 3.5 \times 10^{-12}$  GeV, and (E)  $\Lambda = 4.0 \times 10^{-12}$  GeV. Notice that the Points A – E are indicated in Fig. 5.

quintessence field normalized by  $\rho_Q$

$$\tilde{\delta}_Q = \frac{\delta\rho_Q}{\rho_Q} = \frac{\dot{Q}\dot{\tilde{q}} + V'\tilde{q}}{\rho_Q}. \quad (4.8)$$

For the isocurvature contribution, the energy density perturbation is dominated by that of the quintessence and hence it induces the metric perturbation  $\Psi$ . This becomes a source of the CMB anisotropy through the Sachs-Wolfe effect. When the slow-roll condition is satisfied for the quintessence,  $\tilde{\delta}_Q(k)$  is approximated as

$$\tilde{\delta}_Q \simeq \frac{V'}{\rho_Q} \left( -\frac{2\dot{\tilde{q}}}{9H} + \tilde{q} \right), \quad (4.9)$$

and it changes its behavior at the scale  $k_{\text{phys}} \sim H_0$  or at  $k_{\text{phys}} \sim \Lambda^2/f_Q$ , as a consequence of the scale dependence of  $\tilde{q}$ .

Now, we consider the CMB anisotropy in the case with the isocurvature mode. We calculate the CMB anisotropy for various cases, and in Table 1, we show the quadrupole  $C_2$  normalized by  $C_{10}$ .

If we limit ourselves to the parameter region which is consistent with the COBE, BOOMERanG, and MAXIMA observations with simple scale-invariant primordial fluctuation, effect of the isocurvature mode is quite small as far as  $r_q \lesssim 1$ . This is because, in such cases, there is a severe upper bound on  $\Lambda$  to suppress the late time ISW effect which enhances  $C_l$  with small  $l$ . As a result, the quintessence field cannot dominate the universe when  $z \gg 1$ . Then, the isocurvature fluctuation in the quintessence density also becomes a minor effect until very recently. As one can see in Table 1, for the best-fit value of  $\Lambda$  (i.e., for the Point A given in Fig. 5), the enhancement of  $C_2$  is about 2 % even for  $r_Q = 2$ . If we consider larger value of  $\Lambda$ , effect on  $C_2$  is more enhanced. For  $(f_Q, \Lambda) = (5 \times 10^{17} \text{ GeV}, 3.0 \times 10^{-12} \text{ GeV})$  (i.e., for the Point C given in Fig. 5, which is allowed at 99 % C.L.), we calculate the CMB angular power spectrum and the result is given in Fig. 8. In this case,  $C_2$  can be enhanced by the factor 2.6 if  $r_Q = 2$ .

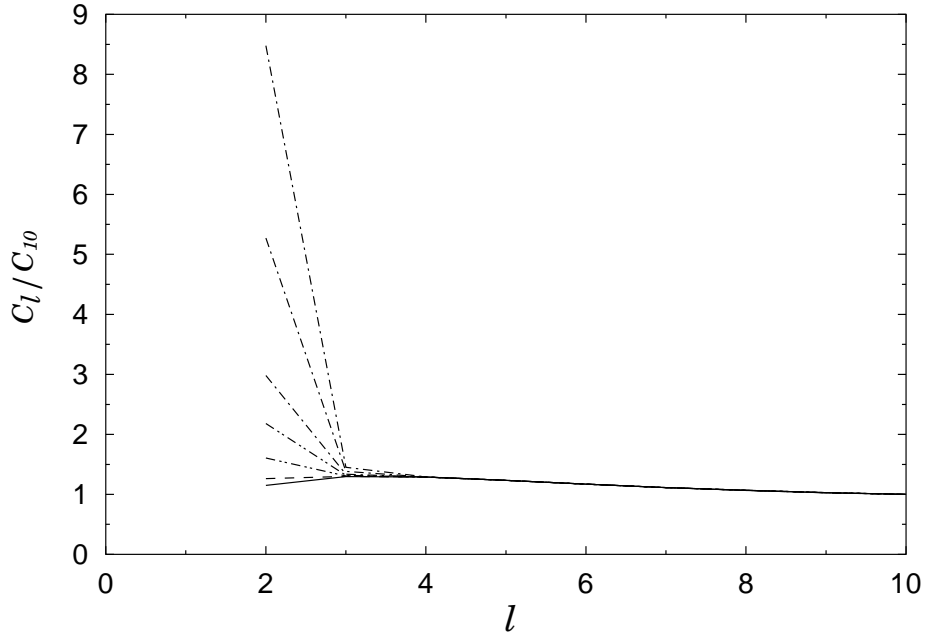


Figure 8:  $C_l/C_{10}$  for  $r_q = 0, 0.5, 1, 1.5, 2, 3,$  and  $4$  from below with  $f_Q = 5 \times 10^{17}$  GeV and  $\Lambda = 3.0 \times 10^{-12}$  GeV.

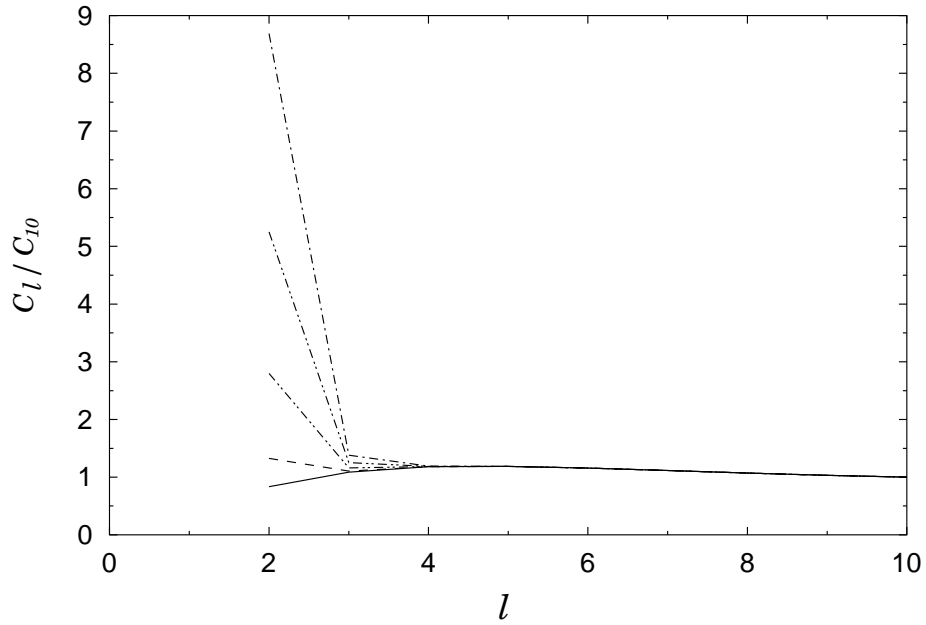


Figure 9:  $C_l/C_{10}$  for  $r_q = 0, 0.5, 1, 1.5,$  and  $2$  from below with  $f_Q = 5 \times 10^{17}$  GeV and  $\Lambda = 3.5 \times 10^{-12}$  GeV.

One should note that angular power spectrum of the CMB anisotropy strongly depends on the primordial spectrum of the fluctuations. Thus, the constraint on the  $f_Q$  vs.  $\Lambda$  plane is sensitive to the scale-dependence of the primordial adiabatic fluctuation which is determined by the model of the inflation. Therefore, if we adopt a possibility of a non-trivial scale dependence of the primordial fluctuation, the constraint on the  $f_Q$  vs.  $\Lambda$  plane given in the previous section may be relaxed or modified. If this is the case, larger value of  $\Lambda$  may be allowed and the energy density of the quintessence field may become significant at earlier stage of the universe. Thus, we also consider such cases. In Fig. 9, we plot  $C_l$  normalized by  $C_{10}$  for  $(f_Q, \Lambda) = (5 \times 10^{17} \text{ GeV}, 3.5 \times 10^{-12} \text{ GeV})$ . In addition, in Table 1, the ratio  $C_2/C_{10}$  is shown for the Points D and E. As one can see, effect on  $C_2$  is much more significant than the previous case.

At low multipoles the uncertainty of the CMB data is dominated by “cosmic variance.” For  $C_2$  which is mostly enhanced by the isocurvature fluctuations, the cosmic variance gives  $\sqrt{2/5} \simeq 60\%$  error to observation.<sup>#7</sup> Thus, it is difficult to see the effect of the isocurvature mode when  $r_q \lesssim 1$  if the quintessence field does not oscillate so much until the present epoch. However, if a large value of  $\Lambda$  is possible, the isocurvature effects may be detectable even with  $r_q \gtrsim 0.5$ , which is realized, for example, in the chaotic inflation model with  $V_{\text{inf}} \propto \chi^p$  with  $p \gtrsim 8$  (see, for example, Point E in Table 1).

## 5 Conclusions and Discussion

We have studied the CMB anisotropies produced by cosine-type quintessence models. In particular, effects of the adiabatic and isocurvature fluctuations have been both discussed.

For purely adiabatic fluctuations with scale invariant spectrum, the existence of the quintessence suppresses the relative height of the first acoustic peak of the angular power spectrum compared with the  $\Lambda$ CDM case. This is because, in the quintessence models, the “dark energy” due to the quintessence may dominate the universe earlier than the cosmological constant case, and hence the late time ISW effect becomes more effective. As a result, the CMB anisotropy for large angular scale is more enhanced, which relatively suppresses the height of the acoustic peaks. Because of this effect, we have seen that the CMB data from COBE, BOOMERanG and MAXIMA have imposed the stringent constraint on the model parameters of the quintessence models. We have also seen that the location of the the first acoustic peak shifts to lower multipole  $l$  compared with  $\Lambda$ CDM models.

In the case of the cosine-type quintessence models, the quintessence field has a negligible effective mass during inflation and hence its amplitude may acquire sizable fluctuation due to the quantum fluctuation in the de Sitter background. Such a fluctuation becomes isocurvature fluctuation. We have shown that the isocurvature fluctuations have significant effects on the CMB angular power spectrum at low multipoles in some parameter space,

---

<sup>#7</sup>The measurement of the CMB polarization toward many clusters would allow some further reduction of the cosmic variance [21].

which may be detectable in future satellite experiments. In the tracker-type models, the quintessence field has a larger effective mass than the Hubble parameter in the early universe, and hence the isocurvature fluctuations are dumped away as the quintessence field evolves following the attractor point. Consequently, we cannot expect to see the effect of the isocurvature fluctuation in the tracker case. Therefore, the effect of isocurvature fluctuations on the CMB spectrum may be important to distinguish two types of the quintessence models.

Since very accurate measurements of the CMB anisotropy are expected in the near future, in particular by the MAP [22] and PLANCK [23] experiments, we will have more stringent constraints on the quintessence models as well as on the  $\Lambda$ CDM models. Importantly, the quintessence and  $\Lambda$ CDM models may have different predictions on the shape of the CMB angular power spectrum, and some of the models may be confirmed or excluded once better observations of the CMB anisotropy become available. In particular, in the cosine-type quintessence models, we have seen that the isocurvature perturbation may enhance the CMB angular power spectrum at low multipoles (in particular,  $C_2$ ), which may be an interesting signal of the cosine-type quintessence models.

*Acknowledgment:* M.K. thanks N. Sugiyama for useful discussion. This work is supported by the Grant-in-Aid for Scientific Research from the Ministry of Education, Science, Sports, and Culture of Japan, No. 12047201, No. 13740138 and Priority Area ‘‘Supersymmetry and Unified Theory of Elementary Particles’’ (No. 707).

## References

- [1] P. de Bernardis et al., Nature **404** (2000) 995.
- [2] S. Hanany et al., astro-ph/0005123.
- [3] B. Ratra and P.J.E. Peebles, Phys. Rev. **D37** (1988) 3406;  
 P.G. Ferreira and M. Joyce, Phys. Rev. **D58** (1998) 023503;  
 I. Zlatev, L. Wang and P.J. Steinhardt, Phys. Rev. Lett. **82** (1999) 896;  
 P.J. Steinhardt, L. Wang and I. Zlatev, Phys. Rev. **D59** (1999) 123504;  
 P. Brax and J. Martin, Phys. Lett. **B468** (1999) 40; Phys. Rev. **D61** (2000) 103502;  
 T. Barreiro, E.J. Copeland and N.J. Nunes, Phys. Rev. **D61** (2000) 127301.
- [4] J.E. Kim, JHEP **9905** (1999) 022;  
 Y. Nomura, T. Watari and T. Yanagida, Phys. Lett. **B484** (2000) 103; Phys. Rev. **D61** (2000) 105007.
- [5] R.R. Caldwell, R. Dave and P.J. Steinhardt, Phys. Rev. Lett. **80** (1998) 1582;  
 S.M. Carroll, Phys. Rev. Lett. **81** (1998) 3067;  
 T. Chiba, Phys. Rev. **D60** (1999) 083508;  
 L. Wang, R.R. Caldwell, J.P. Ostriker and P.J. Steinhardt, Astrophys. J. **530** (2000) 17;

- P. Brax, J. Martin and A. Riazuelo, Phys. Rev. **D62** (2000) 103505;  
 C. Skordis and A. Albrecht, astro-ph/0012195.
- [6] A. Masiero, M. Pietroni and F. Rosati, Phys. Rev. **D61** (2000) 023504;  
 T. Barreiro, E.J. Copeland and N.J. Nunes, Phys. Rev. **D61** (2000) 127301;  
 E.J. Copeland, N.J. Nunes and F. Rosati, Phys. Rev. **D62** (2000) 123503.
- [7] R.K. Sachs and A.M. Wolfe, Astrophys. J. **147** (1967) 73.
- [8] P. Brax, J. Martin and A. Riazuelo, in Ref. [5];  
 M. Kamionkowski and A. Kosowsky, Ann. Rev. Nucl. Part. Sci. **49** (1999)77;  
 M. Doran, M.J. Lilley, J. Schwindt and C. Wetterich, astro-ph/0012139.
- [9] L.R. Abramo and F. Finelli, astro-ph/0101014.
- [10] S. Perlmutter et al., Astrophys. J. **517** (1999) 565.
- [11] I. Dominguez, P. Hoeflich, O. Straniero and C. Wheeler, astro-ph/9905047;  
 P.S. Drell, T.J. Loredo and I. Wasserman, astro-ph/9905027;  
 A.N. Aguirre, astro-ph/9904319;  
 A.G. Riess, A.V. Filippenko, W. Li and B.P. Schmidt, astro-ph/9907038.
- [12] T.S. Bunch and P.C.W. Davis, Proc. Roy. Soc. London **A360** (1978) 117.
- [13] J.M. Bardeen, P.J. Steinhardt and M.S. Turner, Phys. Rev. **D28** (1983) 629.
- [14] U. Seljak and M. Zaldarriaga, Astrophys. J. **469** (1996) 437.
- [15] C. Bennett et al., Astrophys. J. Lett. **464** (1996) L1.
- [16] J.R. Bond, A.H. Jaffe and L. Knox, Astrophys. J. **533** (2000) 19.
- [17] A.H. Jaffe et al., Phys. Rev. Lett. **86** (2001) 3475.
- [18] See RADPACK homepage, <http://flight.uchicago.edu/knox/radpack.html>.
- [19] M. Tegmark and A.J.S. Hamilton, astro-ph/9702019.
- [20] W. Hu and N. Sugiyama, Astrophys. J. **444** (1995) 489; Astrophys. J. **471** (1996) 542.
- [21] M. Kamionkowski and A. Loeb, Phys. Rev. **D 56** (1997) 4511.
- [22] MAP homepage, <http://map.gsfc.nasa.gov/>.
- [23] PLANCK homepage, <http://astro.estec.esa.nl/SA-general/Projects/Planck>.